JOM, Vol. 64, No. 7, 2012
DOI: 10.1007/s11837-012-0349-6

Overview of Amorphous and Nanocrystalline Magnetocaloric Materials Operating Near Room Temperature

HUSEYIN UCAR,[1,3] JOHN J. IPUS,[2] V. FRANCO,[2] M. E. McHENRY,[1] and D. E. LAUGHLIN[1]

1.—Department of Materials Science and Engineering, Carnegie Mellon University, Pittsburgh, PA 15213, USA. 2.—Dpto. Física de la Materia Condensada, ICMSE-CSIC, Universidad de Sevilla, Seville, Spain. 3.—e-mail: hucar@andrew.cmu.edu

The observation of a giant magnetocaloric effect in $Gd_5Ge_{1.9}Si_2Fe_{0.1}$ has stimulated the magnetocaloric research in the last two decades. However, the high price of Gd and its proclivity to corrosion of these compounds have prevented their commercial use. To reduce raw materials cost, transition metal-based alloys are investigated to replace rare earth-based materials. Environmental considerations, substitution for scarce and strategic elements, and cost considerations all speak to potential contributions of these new materials to sustainability. Fe-based soft amorphous alloys are believed to be promising magnetic refrigerants. Efforts in improving the refrigeration capacity (RC) of refrigerants mainly rely on broadening the magnetic entropy change. One promising technique is to couple two phases of magnetic materials with desirable properties. Second is the investigation of nanoparticle synthesis routes, with ball milling being the most widely used one. The motivation for the nanoparticles synthesis is rooted in their inherent tendency to have distributed exchange coupling, which will broaden the magnetic entropy curve. As proven with the cost analysis, the focus is believed to shift from improving the RC of refrigerants toward finding the most economically advantageous magnetic refrigerant with the highest performance.

BACKGROUND

In the last decade, there has been an increased interest in magnetocaloric materials. Among many of the applications, the current interest has been on magnetic refrigeration near room temperature because this technology is energetically more efficient than that based on conventional gas compression refrigeration, by about 20%.[1,2] Besides being energetically more favorable, magnetocaloric materials are also more environmentally friendly because ozone-depleting and global warming gases are not used.

Besides magnetic refrigeration, heat engines and heat pumps are some other applications that rely on the same property. Magnetocaloric materials can be tailored depending on the needs of each application, which can lead to efficient and profitable use of thermodynamic cycles. This article provides an overview of the current state of the art of magnetocaloric materials with an emphasis on the importance of metastable γ-FeNi-based nanocomposites and Fe-based amorphous alloys. First, rare earth magnetocaloric materials are presented, which is followed by Fe-based amorphous alloys. Then, a detailed analysis of γ-FeNi system regarding its microstructural and magnetocaloric properties is given.

MAGNETOCALORIC EFFECT AND EQUATIONS OF STATE

The magnetocaloric effect (MCE) was first described by Warburg.[3] MCE provides a unique way for realizing refrigeration from ultra-low temperatures to room temperature. Interesting MCE materials that can rely on nanostructures include paramagnetic salts used for attaining low temperatures,[4,5] and superparamagnetic particles[6] for intermediate temperatures. Materials, with transitions at room temperature and higher, rely on ferromagnetic to paramagnetic or magnetostructural phase transformations.

(Published online June 29, 2012)

The MCE is a property of magnetic materials and is manifested in the reversible heating or cooling of a magnetic material after the application of a magnetic field. On adiabatic magnetization of a material, the entropy of the spin subsystem decreases, leading to the heating of the material, and when this magnetic field is removed adiabatically, the material is cooled.[7] The magnetic entropy change due to the application of a magnetic field H is determined from temperature- and field-dependent magnetization curves by integrating the magnetic Maxwell relation

$$\Delta S_{\mathrm{M}} = \int_0^{H_{\max}} \left(\frac{\partial M}{\partial T}\right)_H \mathrm{d}H \qquad (1)$$

where ΔS_{M} is the magnetic entropy change, M is the magnetization, and T is the temperature.

Magnetocaloric materials can be divided in two classes based on the type of phase transition: (I) first-order magnetostructural phase transition and (II) second-order magnetic transition. The first type, called giant magnetocaloric effect materials, exhibit a large and narrow peak magnetic entropy change accompanying a magnetostructural phase transition, but this is often accompanied by undesirable thermal hysteresis.[8–10] Materials with a second-order magnetic phase transition usually show a lower peak entropy change but with a broader peak, which results in an enhanced refrigerant capacity.[11,12] Moreover, these materials present reduced hysteresis loss and tunable Curie temperatures.[13,14]

For materials with second-order phase transition, Arrott and Noakes proposed the following equation of state that describes the magnetic response of a material around its critical temperature.[15]

$$H^{1/\gamma} = a(T - T_{\mathrm{C}})M^{1/\gamma} + bM^{1/\beta+1/\gamma} \qquad (2)$$

where β and γ are critical exponents describing the temperature dependence of magnetization and inverse susceptibility, respectively. When mean field arguments failed to explain the field dependence of peak magnetic entropy change ΔS_{M} for materials with second-order transition, Franco and Conde[16] proposed to use Arrott-Noakes equation of state. The field dependence of the magnetic entropy change can be expressed as $|\Delta S_{\mathrm{M}}^{\mathrm{pk}}| \propto H^n$, with an exponent $n = 2/3$ for the mean field case.[17] However, this value of the exponent often deviates from experimental observations for soft magnetic materials, and it has been proven that, for a general case, an exponent governing the field dependence of $|\Delta S_{\mathrm{M}}^{\mathrm{pk}}|$ is related to the critical exponents in the following way[16]:

$$n = 1 + \frac{\beta - 1}{\beta + \gamma} \qquad (3)$$

where β and γ can be obtained through fitting experimental results as described in the following. After determining the Curie temperature T_{C} of the alloy of interest, isothermal magnetization curves are obtained every 2 K in the proximity of T_{C}. The extrapolation of the high-field portion of the $M^{2.5}$ versus $(H/M)^{0.75}$ curves is used to obtain the spontaneous magnetization and initial susceptibility from the intercepts with the $(H/M)^{0.75} = 0$ and $M^{2.5} = 0$ axes, respectively.[18] These values were subsequently processed following the Kouvel-Fisher method[19] to obtain the critical exponents and a precise determination of T_{C}. The predicted and experimental field dependence of the magnetic entropy change curves were proven to be in good agreement for soft magnetic materials with second-order phase transition.[12,13] However, one should keep in mind that this technique is not suitable for biphasic materials or materials with first-order transition.

The Arrott-Noakes equation is accurate in describing and predicting the $M(T)$ near the transition temperature, but this is not the case at lower temperatures. Gallagher et al.[20] modified the Handrich-Kobe equation by introducing two asymmetric exchange fluctuation parameters, δ_+ and δ_-, yielding Eq. 4

$$\sigma(T) = \frac{1}{2}\{B_{\mathrm{s}}[(1 + \delta_+)x] + B_{\mathrm{s}}[(1 - \delta_-)x]\} \qquad (4)$$

Here, the disorder of the alloy is taken into consideration by assuming asymmetric exchange interactions present in the amorphous matrix of the nanocomposite alloy. This equation well describes the $M(T)$ at low temperatures. However, it is insufficient for the regime where the transition from ferromagnetic to paramagnetic phases occurs. Recently, Jones et al.[21] combined the two equations of state to obtain a complete description of the magnetic response of the soft magnetic materials. The idea of combining the two models is to bring both the low temperature accuracy and disorder within the context of a modified Brillouin function and the Curie tail together into one curve. With this model, the goal is to determine role of disorder and distributed magnetic exchange interactions in metastable nanostructures for applications in magnetocaloric cooling near room temperature. An example of the entropy curve calculated from the actual data is shown in Fig. 1. Experimental data were obtained from $(Fe_{70}Ni_{30})_{88}Zr_7B_4Cu_1$ alloy. Ball-milled powder was annealed at 700°C and quenched in water to stabilize the metastable γ-FeNi phase. The combined fit presented gives a more realistic measure of the actual behavior of the material in a broader temperature range compared with the fit from Arrott-Noakes, which displays a plateau at low temperatures, leading to an overestimation of refrigeration capacity (RC).

SURVEY OF MATERIALS

This section includes the current state of the art of magnetocaloric materials and compares their

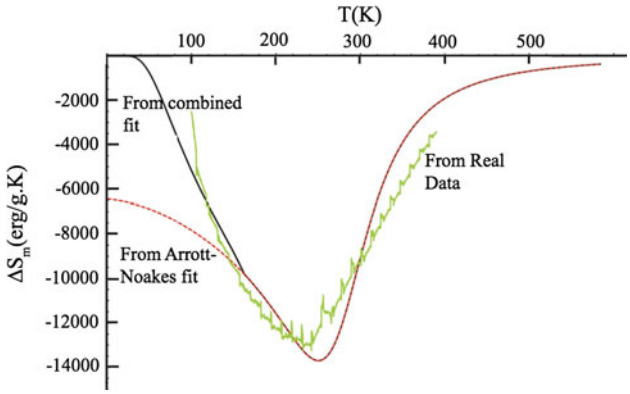

Fig. 1. (color online) Change in entropy integrated from figure with H_{max} at 5T using just the Arrott-Noakes equation (red dashed), the combined fit (black), and averaged experimental data obtained from $(Fe_{70}Ni_{30})_{88}Zr_7B_4Cu_1$ alloy (green).

operating temperature, magnetocaloric response, and synthesis routes. The magnetocaloric response of materials is compared by a parameter called RC. However, there are different definitions of RC in the literature. Therefore, it is crucial to compare the same RC types to avoid ambiguity. One early and widely used definition is given by Wood and Potter[22] where the refrigerant capacity for a reversible refrigeration cycle operating between TH (the temperature of the hot reservoir) and TC (the temperature of the cold reservoir) corresponds to the largest rectangle that can be inscribed inside the $\Delta S_M(T)$ curve, i.e., $RC_{WP} = \Delta S_M \Delta T$, with ΔS_M the magnetic entropy change at the hot and cold ends of the cycle and $\Delta T = TH - TC$. According to Wood and Potter's definition, both the peak magnitude and width are equally important, thus making them suitable metrics for comparing different alloys. Another well-known definition of RC is the product of the peak entropy change times the full width at half maximum (FWHM) of the peak ΔT, $RC_{FWHM} = |\Delta S_M^{pk}| \Delta T$. The third is value is designated as RC_{AREA}, which is calculated by integrating ΔS_M across the temperature range spanning the half maximum of the entropy change. When comparing different materials, the method that is used to calculate the RC will be specified to avoid confusion. Another confusion when comparing materials arises due to the differences in the experimental capabilities from one laboratory to another. Researchers tend to present their work at the maximum field they can achieve, which causes difficulties when comparing. This is why understanding the field dependence of ΔS_M and of RC is crucial, and it has been proven that it also scales with field following a power law.[16] That way, one can extrapolate these metrics of a magnetocaloric material to magnetic fields where comparison with other benchmark materials is possible.

The significance of nanostructured powders is the fact that these powders have a distribution of magnetic transition close to room temperature and a broader temperature dependence of magnetic entropy change, giving larger temperature span in magnetic refrigeration. Moreover, nanoparticles are easy to suspend in the solutions thus providing versatility in practical applications.

The processing routes used to synthesize desirable microstructures are (I) plasma torch synthesis of alloy nanopowders, (II) chemical methods, (III) nanocrystallization of melt spun amorphous precursor followed by primary crystallization to yield nanocrystals of a phase with an appropriate Curie temperature, and (IV) ball milling of the powders to produce nanopowders. Nanocrystalline structures can be obtained via these four processing routes. However, nanostructured magnetocaloric refrigerants presented in this overview are produced either via melt spinning or ball milling. Plasma torch synthesis,[23] however, is a high-throughput method for producing magnetic nanoparticles, which makes it promising for industrial use. A wide variety of starting materials and reactant gases can be used as feedstocks, and many classes of materials, including metals, alloys, carbides, and nitrides can be synthesized. In chemical synthesis, metal salt, a reducing agent and a stabilizer are mixed to produce metal nanoparticles. The reducing agent detaches metal from the salt and the stabilizer passivates the nanoparticle to suppress further growth of the nuclei. This technique is a preferable alternative for producing monodisperse nanoparticles.

Amorphous metallic alloys are synthesized by rapid solidification processing techniques in alloy systems where the liquid phase remains stable to low temperature and there are competing crystalline phases below the liquidus, i.e., systems with deep eutectics. Melt spinning is deemed one type of rapid solidification routes where cooling rates of 10^4 K/s are achieved. This technique yields amorphous metallic ribbons typically 20 μm in thickness. Here, a molten alloy is pushed through a nozzle of a pressurized crucible onto a rotating copper wheel. FINEMET, Fe-Si-B; NANOPERM, FeZrB; and HITPERM, FeCoZrB are three well-known compositions required to fabricate amorphous precursors for nanostructured materials.[24]

Another common method is mechanical alloying (MA), which is a solid-state powder processing technique involving repeated welding, fracturing, and rewelding of powder particles in a high-energy ball mill.[25] With this technique, one can produce amorphous, quasicrystalline structures as well as nanostructures in elements and solid solutions.[26–28] Solid solutions can also be supersaturated considerably compared with the thermodynamic equilibrium by such processing. Here, FINEMET, NANOPERM, and HITPERM types of alloys also yield amorphous structures. One disadvantage of MA is that high-energy ball milling generates heat due to grinding of balls against the powder, which could lead to form agglomerates, increasing the powder particle size. To avoid excessive heating,

mill should be performed intermittently in an inert atmosphere, which in turn will avoid the formation of oxides in the milled powder. Another disadvantage is the poor control over final compositions. During milling, the possibility of contamination due to the interaction of the powder with the wall of the vial is very high. This might lead to undesired changes in the final composition.

This overview is aimed to focus on amorphous and nanocrystalline magnetocaloric materials that operate near room temperature. However, other significant magnetic refrigerants are also presented where appropriate. As mentioned in the beginning, materials with a giant magnetocaloric response are accompanied by an undesirable thermal hysteresis. Provenzano et al.[9] addressed this problem in their study on $Gd_5Ge_2Si_2$ system. They found that small additions of Fe significantly decrease hysteresis losses. However, this is at the expense of changing the order of the phase transition from first order to second order. Despite that the peak entropy change decreased with respect to the undoped compound, the net refrigerant capacity was considerably enhanced. Therefore, $Gd_5Ge_{1.9}Si_2Fe_{0.1}$ was considered a benchmark magnetocaloric refrigerant near room temperature and stimulated the further studies on magnetocaloric refrigeration.

Rajkumar et al.[29] ball milled the annealed ingots of $Gd_5Ge_{1.9}Si_2Fe_{0.1}$ and $Gd_5Ge_2Si_2$. However, ball-milled $Gd_5Ge_{1.9}Si_2Fe_{0.1}$ was found to have a lower RC value than its counterpart $Gd_5Ge_{1.9}Si_2Fe_{0.1}$ from Provenzano's study.[9] This could be due to the differences in the production methods used in each study. Those skilled in the art will recognize that even though this alloy has a high refrigerant capacity, the price associated with the production of it makes this alloy a less desirable magnetic refrigerant. Therefore, it is important to find new magnetic refrigerants that are cheap and will facilitate industrial scale up.

In an effort to reduce the cost, researchers started investigating the applicability of soft amorphous alloys as magnetic refrigerants.[12,30–36] Besides having low cost and reduced hysteresis losses, tunable T_c of soft amorphous alloys are the main reasons for studying these materials. The tunability of T_c is studied by Franco et al.,[37] where they showed that small increases in B content in FeMoCuB alloy significantly changes the T_c without altering the $|\Delta S_M^{pk}|$ of the magnetic entropy curve.

Law et al.[38] studied the effect of Gd on Fe-B-Cr amorphous alloys and investigated the possibility to tune the T_c with small inclusions of Gd. Small additions of Gd was shown to allow tuning the T_c and enhancing thermal stability. The best magnetocaloric response of this series was observed for the $Fe_{79}B_{12}Cr_8Gd_1$, which exhibited larger RC than the benchmark alloy $Gd_5Ge_{1.9}Si_2Fe_{0.1}$. Caballero-Flores et al.[39] showed that the combined addition of Co and Ni to $Fe_{88-x}Zr_7B_4Cu_1$ type alloys leads to amorphous materials with large magnetocaloric response, which was superior to the well-known aforementioned magnetic refrigerant $Gd_5Ge_{1.9}Si_2Fe_{0.1}$ by 40% in terms of their RC values with a T_c approximately at room temperature. This series provides the largest RC values among transition metal-based amorphous alloys published so far. In another paper by Caballero-Flores et al., it was argued that combining two phases of an amorphous alloy led to enhanced RC values. Two-phase magnetic composite based on $Fe_{88-x}Co_xNi_xZr_7B_4Cu_1$ amorphous alloys were combined, and an improvement in RC of ≈92% compared with $Gd_5Ge_{1.9}Si_2Fe_{0.1}$ was reported.

Hu et al.[40] investigated the magnetocaloric properties of $LaFe_{11.7}Si_{1.3}$, which exhibited a T_c approximately 188 K. The metamagnetic transition above T_c of this alloy led to significant broadening of the ΔS_M, which consequently increased its RC value. Fujieda et al.[41] modified the alloy composition by means of hydrogen absorption, which increased the T_c from 188 K to 291 K without compromising the magnetocaloric response.

Other room-temperature magnetocaloric refrigerants produced via ball milling are Pr_2Fe_{17} and $Ni_{2.18}Mn_{0.82}Ga$, by Gorría et al.[42] and de Santanna et al.,[43] respectively. These are other promising materials for magnetocaloric refrigerants at approximately room temperature. In another study by Ipus et al.,[14] partial crystallization in Fe-Nb-B was shown to change the T_c of the alloy as a function of the crystalline fraction due to compositional changes in the amorphous matrix, along with the magnetocaloric response. Moreover, amorphous fraction was observed to favor the magnetocaloric response in these soft magnetic nanocrystalline alloys. Another study by Ipus et al.[44] showed that Co addition to Fe-Nb-B alloy delayed the amorphization process and lowered the RC value slightly.

Recently, Ucar et al.[45] synthesized nanostructured γ-FeNi via ball milling with compositions $Fe_{70}Ni_{30}$ and $Fe_{72}Ni_{28}$. In order to obtain a material with a single γ-FeNi phase, the powders were subsequently sealed in a quartz crucible with Ar atmosphere and annealed in the γ-phase region, 700°C, and quenched in water to stabilize the metastable γ-FeNi phase. γ-FeNi of these compositions has peak entropy changes near room temperature, ≈363 K for $Fe_{70}Ni_{30}$ and ≈333 K for $Fe_{72}Ni_{28}$. Moreover, the RC value of $Fe_{70}Ni_{30}$ is comparable with that of promising alloys.[38,39]

Ipus et al.[46] carried out a detailed structural and microstructural characterization for Fe-Ni system that confirmed the extension of the thermal stability of nanostructured γ-FeNi phase to room temperature. One aspect of this work in the context of nanocomposite magnets was in probing the phase evolution during primary nanocrystallization to model its role in determining structural disorder. In that study, high-temperature x-ray diffraction data were taken during nanocrystallization of $(Fe_{70}Ni_{30})_{88}Zr_7B_4Cu_1$ amorphous alloy ribbons. Temperature-dependent XRD patterns showed the

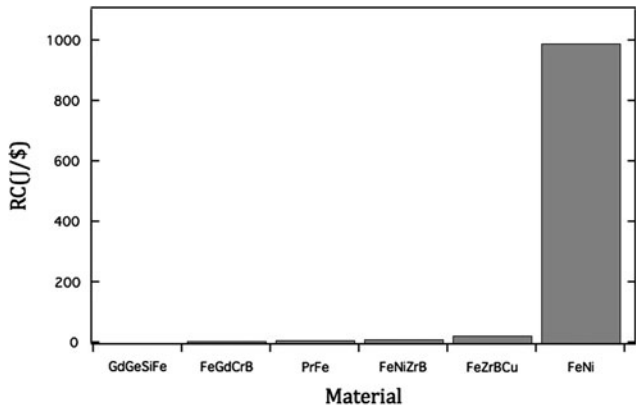

Fig. 2. Refrigeration capacity in J/$ for various magnetocaloric refrigerants.

amorphous phase to be thermally stable to ~673 K where the primary crystallization occurred. The product of the primary crystallization event was a body-centered cubic (bcc) FeNi phase. At increasing temperatures, the phase fraction of bcc FeNi phase was observed to increase and eventually transformed into face-centered cubic phase, which is in agreement with the Fe-Ni phase diagram and previous observations reported for the $Fe_{70}Ni_{30}$ system.[47] Moreover, XRD patterns and magnetic moment measurements on cooling showed the stability of γ-FeNi phase at room temperatures. This makes γ-FeNi phase promising for applications around room temperature.

Miller et al.[48] and McNerny et al.[49] investigated the γ-FeNi nanostructures with tunable Curie temperatures. They obtained Curie temperatures as low as 78°C, which led them to the conclusion that γ-FeNi would impact applications like cancer thermotherapy and polymer curing, which require a low temperature range.

As mentioned before, the cost associated with the production of magnetocaloric refrigerants is a big barrier against industrial scale-up. To have better insight in the economic aspect of this issue, a detailed price analysis is undertaken. In Fig. 2, RC of the most promising magnetic refrigerants with respect to its cost at a field of 5T are compared. The values of RC for these materials are calculated by FWHM method. The results are then divided by the cost per kilogram of the constituent elements of each material. This figure considers not only the magnetocaloric properties but also the prices of each compound. Therefore, it can be used as a means to highlight the most economically advantageous refrigerant with good magnetocaloric properties. For instance, $Gd_5Ge_{1.9}Si_2Fe_{0.1}$, $Fe_{88}Zr_7B_4Cu_1$, and Pr_2Fe_{17} have respectable RC values from the energy standpoint only. However, the prices associated with Gd, Zr, B, and Pr elements lower their RC in terms of J/$ (Fig. 2). In contrast, FeNi is a low-cost compound coupled with good magnetocaloric

Table I. Peak temperature, peak entropy change, RC_{FWHM}, RC_{AREA}, and RC_{WP} values of promising magnetocaloric refrigerants are presented

Nominal composition	T_{pk} (K)	$\lvert\Delta S_M^{pk}\rvert$(1.5$T$) (J kg^{-1} K^{-1})	RC_{FWHM} (1.5T) (J kg^{-1})	RC_{FWHM} (2T) (J kg^{-1})	RC_{FWHM} (5T) (J kg^{-1})	RC_{AREA} (5T) (J kg^{-1})	RC_{WP} (5T) (J kg^{-1})	Refs.
$Gd_5Ge_2Si_2$	240			45				29
$Fe_{75}Nb_{10}B_{15}$	250	0.6	115		445		283	14
$Mn_{1.1}Fe_{0.9}Pe_{0.78}Ge_{0.22}$	280	10			400			50
$Ni_{2.18}Mn_{0.82}Ga$	300			66				43
Pr_2Fe_{17}	300				573			42
$Gd_5Ge_{1.9}Si_2Fe_{0.1}$	300				630	355	240	9
$Fe_{88}Zr_7B_4Cu_1$	300	1.3	166		654	496		39
$Fe_{76}Mo_8Cu_1B_{15}$	315	0.92					180	37
$Fe_{72}Ni_{28}$	333	0.49	73		250			45
$(Fe_{70}Ni_{30})_{89}Zr_7B_4$	342	0.7			330			51
$Fe_{79}Gd_1Cr_8B_{12}$	355	1.42	153		627	459		38
$Fe_{70}Ni_{30}$	363	0.6	158		470			45
$Fe_{78}Co_5Zr_6B_{10}Cu_1$	380	1.6					273	36
$(Fe_{85}Co_{15})_{75}Nb_{10}B_{15}$	440	0.82	102		400			44

properties, which explains the giant response that we see in Fig. 2.

Table I summarizes the magnetocaloric properties of some of the most prominent refrigerants operating near room temperature in the order of increasing peak temperature T_{pk}. Both $Gd_5Ge_{1.9}Si_2Fe_{0.1}$ and $Fe_{88}Zr_7B_4Cu_1$ have slightly higher refrigeration capacities than $Fe_{70}Ni_{30}$. However, when each alloy is considered in terms of the cost associated with their constituent elements, $Fe_{70}Ni_{30}$ alloy is clearly the most economically advantageous refrigerant with good magnetocaloric properties (Fig. 2).

FUTURE TRENDS

The focus in magnetocaloric research seems to be shifting toward materials with nanoscale structures because they exhibit a distributed magnetic transition, which leads to broader magnetic entropy curves with better magnetocaloric refrigerants. However, a good understanding of disorder, surfaces, interfaces, and their role in determining the distribution of magnetic exchange interactions in nanostructures is important, as it will allow tunability of the refrigerant capacity in magnetic nanostructures. This will eventually impact applications in magnetocaloric cooling near room temperature.

In summary, this article reviewed the state of the art of magnetocaloric refrigeration operating near room temperature. This technology relies on a magnetic material's ability to convert magnetic energy into thermal energy and vice versa. The focus is placed on Fe-based alloys and metastable γ-FeNi nanostructures, which have market potential due to having a low price compared to rare-earth materials. Alloys of this type continue to mature and will open new horizons to the growing refrigeration technology in the years ahead.

ACKNOWLEDGEMENTS

H.U., M.E.M., and D.E.L. acknowledge support of the NSF through Grant No. DMR #0804020. J.J.I and V.F. acknowledge the support from the Spanish Ministry of Science and Innovation and EU FEDER (Project MAT 2010-20537), the PAI of the Regional Government of Andalucía (Project P10-FQM-6462) and the United States Office of Naval Research (Project N00014-11-1-0311).

REFERENCES

1. K.A. Gschneidner Jr. and V.K. Pecharsky, *Ann. Rev. Mater. Sci.* 30, 387 (2000).
2. E. Brück, O. Tegus, L. Zhang, X.W. Li, F.R. de Boer, and K.H.J. Buschow, *J. Alloy. Compd.* 383, 32 (2004).
3. M. Untersuchungen and E. Warburg, *Ann. Phys. (Leipzig)* 13, 141 (1881).
4. W.F. Giaque, *J. Am. Chem. Soc.* 49, 1870 (1927).
5. P. Debye, *Ann. Phys. (Leipzig)* 81, 1154 (1926).
6. R. McMichael, R.D. Shull, L.J. Swartzendruber, L.H. Bennett, and R.E. Watson, *J. Magn. Magn. Mater.* 111, 29 (1992).
7. A.M. Tishin and Y.I. Spichkin, *The Magnetocaloric Effect and its Applications* (Bristol, UK: Institute of Physics Publishers, 2003).
8. V.K. Pecharsky and K.A. Gschneidner Jr, *Phys. Rev. Lett.* 78, 4494 (1997).
9. V. Provenzano, A.J. Shapiro, and R.D. Shull, *Nature* 429, 853 (2004).
10. T. Krenke, E. Duman, M. Acet, E.F. Wassermann, X. Moya, L. Mañosa, and A. Planes, *Nat. Mater.* 4, 450 (2005).
11. I. Škorvánek and J. Kovác, *Czech J. Phys.* 54, D189 (2004).
12. V. Franco, J.S. Blázquez, C.F. Conde, and A. Conde, *Appl. Phys. Lett.* 88, 042505 (2006).
13. V. Franco, J.M. Borrego, C.F. Conde, and A. Conde, *J. Appl. Phys.* 100, 083903 (2006).
14. J.J. Ipus, J.S. Blázquez, V. Franco, A. Conde, and L.F. Kiss, *J. Appl. Phys.* 105, 123922 (2009).
15. A. Arrott and J.E. Noakes, *Phys. Rev. Lett.* 19, 786 (1967).
16. V. Franco and A. Conde, *Int. J. Refrig.* 33, 465 (2010).
17. H. Oesterreicher and F.T. Parker, *J. Appl. Phys.* 55, 4334 (1984).
18. V. Franco, J.S. Blázquez, and A. Conde, *Appl. Phys. Lett.* 89, 222512 (2006).
19. J.S. Kouvel and M.E. Fisher, *Phys. Rev.* 136, A1626 (1964).
20. K.A. Gallagher, M.A. Willard, V.N. Zabenkin, D.E. Laughlin, and M.E. McHenry, *J. Appl. Phys.* 85, 5130 (1999).
21. N.J. Jones, H. Ucar, J.J. Ipus, M.E. McHenry, and D.E. Laughlin, *J. Appl. Phys.* 111, 07A334 (2012).
22. M.E. Wood and W.H. Potter, *Cryogenics* 25, 667 (1985).
23. S. Son, M. Taheri, E. Carpenter, V.G. Harris, and M.E. McHenry, *J. Appl. Phys.* 91, 7589 (2002).
24. M.E. McHenry, M.A. Willard, and D.E. Laughlin, *Prog. Mater. Sci.* 44, 291 (1998).
25. C. Suryanarayana, *Prog. Mater. Sci.* 46, 1 (2001).
26. C.C. Koch, O.B. Cavin, G.C. McKamey, and J.O. Scarbrough, *Appl. Phys. Lett.* 43, 1071 (1983).
27. J. Eckert, L. Schultz, and K. Urban, *Appl. Phys. Lett.* 55, 117 (1989).
28. E. Hellstem and L. Schultz, *J. Appl. Phys.* 63, 1408 (1988).
29. D.M. Rajkumar, M. Manivel Raja, R. Gopalan, and V. Chandrasekaran, *J. Magn. Magn. Mater.* 320, 1479 (2008).
30. D. Wang, K. Peng, B. Gu, Z. Han, S. Tang, W. Qin, and Y. Du, *J. Alloys Compd.* 358, 312 (2003).
31. I. Skorvanek and J. Kovac, *Czech J. Phys.* 54, D189 (2004).
32. S. Atalay, H. Gencer, and V.S. Kolat, *J. Non-Cryst. Solids* 351, 2373 (2005).
33. S.G. Min, K.S. Kim, S.C. Yu, H.S. Suh, and S.W. Lee, *J. Appl. Phys.* 97, 10M310 (2005).
34. F. Johnson and R.D. Shull, *J. Appl. Phys.* 99, 08909 (2006).
35. V. Franco, J.S. Blázquez, and A. Conde, *J. Appl. Phys.* 100, 064307 (2006).
36. V. Franco, J.S. Blázquez, M. Millán, J.M. Borrego, C.F. Conde, and A. Conde, *J. Appl. Phys.* 101, 09C503 (2007).
37. V. Franco, C.F. Conde, J.S. Blázquez, and A. Conde, *J. Appl. Phys.* 101, 093903 (2007).
38. J.Y. Law, R.V. Ramanujan, and V. Franco, *J. Alloy. Compd.* 508, 14 (2010).
39. R. Caballero-Flores, V. Franco, A. Conde, K.E. Knipling, and M.A. Willard, *Appl. Phys. Lett.* 96, 182506 (2010).
40. F.X. Hu, M. Ilyn, A.M. Tishin, J.R. Sun, and G.J. Wang, *J. Appl. Phys.* 93, 5503 (2003).
41. S. Fujieda, A. Fujita, and K. Fukamichi, *Appl. Phys. Lett.* 81, 1276 (2002).
42. P. Gorría, J.L. Sánchez-Lamazares, P. Alvarez, M.J. Pérez, J. Sanchez-Marcos, and J.A. Blanco, *J. Phys. D Appl. Phys.* 41, 192003 (2008).
43. Y.V.B. de Santanna, M.A.C. de Melo, I.A. Santos, A.A. Coelho, S. Gama, and L.F. Cótica, *Solid State Commun.* 148, 289 (2008).
44. J.J. Ipus, J.S. Blázquez, V. Franco, and A. Conde, *J. Alloy. Compd.* 496, 7 (2010).
45. H. Ucar, J.J. Ipus, M.E. McHenry, and D.E. Laughlin (unpublished work, 2012).

46. J.J. Ipus, P. Herre, P. Ohodnicki, and M.E. McHenry, *J. Appl. Phys.* 111, 07A323 (2012).
47. L.J. Swartzendruber, V.P. Itkin, and C.B. Alcock, *J. Phase Equilib.* 12, 288 (1991).
48. K.J. Miller, M. Sofman, K. McNerny, and M.E. McHenry, *J. Appl. Phys.* 107, 09A305 (2010).
49. K.L. McNerny, Y. Kim, D.E. Laughlin, and M.E. McHenry, *J. Appl. Phys.* 107, 09A312 (2010).
50. W. Dagula and O. Tegus, *IEEE Trans. Magn.* 41, 10 (2005).
51. J.J. Ipus, H. Ucar, and M.E. McHenry, *IEEE Trans. Magn.* 47, 10 (2011).